Int. J. Electrochem. Sci., 15 **(2020)** 2634 – 2647, doi: 10.20964/2020.03.50

International Journal of ELECTROCHEMICAL SCIENCE
www.electrochemsci.org

Mini Review

Peptide Based Noble Metal Nanomaterials for Oxygen Reduction Reaction: A Review

Meng Zong[1,], Zhaoqing Ding[2], Wei He[1], Jing Luo[3] and Zhenghua Tang[2,4,*]*

[1] Chongqing Chemical Industry Vocational College, Chongqing, 401220, P. R. China.
[2] Guangzhou Key Laboratory for Surface Chemistry of Energy Materials, New Energy Research Institute, School of Environment and Energy, South China University of Technology, Guangzhou Higher Education Mega Centre, Guangzhou, 510006, China.
[3] Chongqing University of Science and Technology, Chongqing, 401331, P. R. China.
[4] Guangdong Engineering and Technology Research Center for Surface Chemistry of Energy Materials, School of Environment and Energy, South China University of Technology, Guangzhou Higher Education Mega Centre, Guangzhou, Guangdong, 510006, P. R. China
[*]E-mail: ahzmeng@126.com, zhht@scut.edu.cn

Received: 30 October 2019 / *Accepted:* 4 January 2020 / *Published:* 10 February 2020

Green energy devices including proton exchange membrane fuel cells (PEMFCs) and rechargeable metal air batteries (RMABs), play a significant role in ameliorating global energy scarcity and severe environment pollution issues. Unfortunately, the sluggish oxygen reduction reaction (ORR) occurring at the cathode restrains the deployment and advancement of PEMFCs and RMABs. Commercial Pt/C catalyst embraces excellent ORR performance but suffers from high cost, limited platinum reserve, as well as undesirable stability and durability. Recently, peptide-based noble metal nanomaterials with distinguished activity and robust durability have been emerging as a new type of ORR catalyst, as the preparation of such catalyst is environmentally friendly, and peptide can manipulate the physical, chemical and electronic properties of the catalyst with desirable functionalities. In this review, the basic principle and mechanism regarding ORR are firstly introduced and discussed, along with the recent progresses of peptide-based nanomaterials. Afterwards, we systematically summarize the achievements regarding employing peptide as template to prepare single noble metal, alloyed bimetallic, and core-shell bimetallic nanomaterials for achieving improved ORR activity and stability. In the end, the ascendancies, challenges and perspectives in this flourishing realm will be expounded, with an emphasis on the great potentials and opportunities to engineer peptide-based noble metal nanomaterials as high-efficiency and durable catalysts for ORR and other electrochemical energy applications.

Keywords: Peptide sequence; Noble metal nanomaterials; Oxygen reduction reaction; Proton exchange membrane fuel cell; Rechargeable metal-air batteries

1. INTRODUCTION

1.1. The significance and associated mechanism of ORR

Presently, the rapidly dwindling supply of fossil fuels and exacerbation of global warming have appreciably irritated the development of clean and sustainable energy devices, including proton exchange membrane fuel cells (PEMFCs), rechargeable metal-air batteries (RMABs) and so on.[1-3] Notably, the oxygen reduction reaction (ORR) underpins the above green energy devices and possesses a critical role in the field of electrocatalysis.[4, 5] As for PEMFCs and RMABs, the shortage of highly efficient ORR catalyst significantly restricts the overall efficiency.[6-8] It is well acknowledged that, commercial Pt/C (20 *wt.* %) is the state-of-the-art catalyst for ORR with "incomparable" performance. Nevertheless, the abundance of platinum in Earth's Crust is considerably scarce and so-caused high cost, plus the poor long term durability and low poison resistance of the Pt/C catalyst, all these factors result in its large-scale deployment being harshly impeded.[9-12] Therefore, the design and preparation of high-efficiency, cost effective and robust electrocatalysts for ORR have been a long-pursuing goal in this field.

In the ORR process, molecular oxygen is electrochemically reduced by protons and electrons to form water eventually, which is associated with the generation of an electrical potential.[13] The practical reduction processes of O_2 in aqueous electrolytes are complicated and markedly different in acidic and alkalic medium, as summarized in equations (1-8):[14, 15]

Acidic medium:

$$O_2 + 4H^+ + 4e^- \rightarrow 2H_2O \quad (1)$$

$$O_2 + 2H^+ + 2e^- \rightarrow H_2O_2 \quad (2)$$

$$H_2O_2 + 2H^+ + 2e^- \rightarrow 2H_2O \quad (3)$$

$$2H_2O_2 \rightarrow 2H_2O + O_2 \quad (4)$$

Alkaline medium:

$$O_2 + 2H_2O + 4e^- \rightarrow 4OH^- \quad (5)$$

$$O_2 + H_2O + 2e^- \rightarrow HO_2^- + OH^- \quad (6)$$

$$HO_2^- + H_2O + 2e^- \rightarrow 3OH^- \quad (7)$$

$$2HO_2^- \rightarrow 2OH^- + O_2 \quad (8)$$

Taking fuel cells as an example, when O_2 is reduced by the galvanic system, the maximum free energy is harnessed with O_2 reduced by the four-electron transfer pathway (1 and 5). The O_2 reduced by the two-electron pathway (2 and 6) offers only about half the energy of the four-electron process.[15] And the two-electron pathway usually occurs to generate H_2O_2 or HO_2^- first, accompanied by the further reduction to form H_2O or OH^-.

The overall ORR course includes either $4e^-$ or two-step $2e^-$ reduction pathway.[16] In practical PEMFCs and RMABs operations, a direct four-electron path is extremely desirable for the purpose of ideally high efficiency, while selective two-electron reduction is also acceptable in some cases and can be applied into industrial production of H_2O_2.[16, 17] The intrinsic ORR mechanisms are complex and distinct, which rely upon the surface atomic structure of the catalysts. For the $4e^-$ pathway, there are also two possible processes (dissociative and associative pathways) with similar mechanisms in acidic and

basic media. The concerning mechanisms in basic electrolyte can be summarized by the equations (9-11):[18]

Dissociative mechanism:

$O_2 + 2* \rightarrow 2O*$ (9)

$2O* + 2e^- + 2H_2O \rightarrow 2OH* + 2OH^-$ (10)

$2OH* + 2e^- \rightarrow 2OH^- + 2*$ (11)

where * represents the reaction active site on the surface of the catalyst. The specific process is that, O_2 is adsorbed originally, and then the O–O bond is broken into two adsorbed atomic O* species, which subsequently acquire two protons and $2e^-$ to form OH* and further generate OH^- eventually.

Meanwhile, ORR can also proceed on the basis of the associative mechanism involving two-electron or four-electron route:

The two-electron route:

$O_2 + * \rightarrow O_2*$ (12)

$O_2* + H_2O + e^- \rightarrow OOH* + OH^-$ (13)

$OOH* + e^- \rightarrow OOH^- + *$ (14)

The four-electron route:

$O_2 + * \rightarrow O_2*$ (15)

$O_2* + H_2O + e \rightarrow OOH* + OH$ (16)

$OOH* + e \rightarrow O* + OH$ (17)

$O* + H_2O + e \rightarrow OH* + OH$ (18)

$OH* + e \rightarrow OH + *$ (19)

Enlightened by the significance and great worthiness of ORR, extensive research endeavors have been dedicated to exploring efficient catalysts toward ORR, such as porous carbon materials,[19] transition metal based nanocomposites,[20, 21] the alloyed bimetallic architecture,[22] the heterostructure nanomaterials,[23] and so on. Recently, employing biomolecules especially peptide as template to direct the formation of noble metal nanomaterials has been gaining more and more research attentions, mainly thanks to the merits including mild preparation conditions, a wide choice of metal substrates, and most importantly, the peptide sequence can impart the catalyst with enhanced activity and superior long term stability.[24, 25]

1.2 The peptide based noble metal nanomaterials for ORR

Peptide-based approach can pave a new avenue for preparing highly efficient electrocatalysts under gentle circumstances based on the following ascendancies: Firstly, the fabrication of peptide-templated nanomaterials is generally executed in water without using toxic organic solvent, at ambient temperature without annealing or hydrothermal treatment, and such process has nearly zero-energy depletion, which are environmentally friendly; more importantly, the peptide sequences can hold specific binding affinities toward targeted metal substrates, and they are able to direct the nuclei growth and nanoparticle formation, hence achieving desirable particle size, shape/morphology, composition, and other designated functionalities.[26-29]

For instance, Dey group reported that the peptide $A\beta_{Cys}$ can form self-assembled adlayers onto the Au surface, which displayed miscellaneous catalytic performances for both ORR and hydrogen evolution reaction.[30] In another study, Wu and co-workers employed peptide Z1 as template/ligand to synthesize alloyed AuPt nanoparticles, which exhibited superior ORR activity to Pt/C and comparable HER reactivity with Pt/C in alkaline media.[28] Recently, Wang *et. al* reported the L-phenylalanine templated preparation of the Pt-AL/C nanostructure through the assistance of electron reduction.[31] Density functional theory (DFT) calculations indicated that the N dopants could stabilize the Pt nanoparticles and reduce the *O/*OH binding energies on the surface of Pt NPs.[31] Consequently, Pt-AL/C exhibited significantly promoted ORR activity and stability over the Pt/C catalyst.[31]

2. ENGINEERED PEPTIDE-BASED NOBLE METAL NANOMATERIALS FOR ORR

In recent years, studies on diverse peptide-templated noble metal nanomaterials have declared that peptide can crucially and selectively direct the growth of precious metal on its binding sites.[32] Confirmed by theoretical computation and experimental verification, such intentions of peptide templets can be attributed to their strong and adjustable interaction with designated metallic surfaces.[33, 34] Therefore, great research endeavors have been dedicated to exploit multiple noble metal nanomaterials based on strong interaction between the metal surface and the peptide sequence, including peptide-templated single precious metal, alloyed bimetallic, and core-shell bimetallic nanomaterials, and so on.

2.1 Peptide-based single noble metal nanomaterials for ORR

In the past decade, peptide sequences with specific binding affinities for various different metal substrates have been identified, including Au, Pd, Pt, Ag, and other noble metals, where the peptide sequence plays a critical role in direct the formation of well-defined single noble metal nanomaterials. For example, Lee *et. al* mimicked the nature by using a biomineralization means to design the growth of inorganic materials, which exhibited excellent ORR performance. To manipulate the nucleation growth of Au nanoparticles, two residues in Hexcoil-Ala were substituted with cysteine to acquire a mutated peptide, HexCoil-Ala-2Cys, which eventually afforded surface atomically well-distributed and size-defined Au nanoparticles.[33] Also, the highly active and stable platinum nanocrystals were prepared by Liu group through a peptide-assisted strategy at ambient temperature for oxygen electroreduction, and the catalyst possessed active sites featuring chiefly at Pt(111) facets with the particle size around 2 nm. The specific and mass activities of the as-prepared Pt (111)-P/C catalyst were nearly twice better than that of Pt/C, and Pt (111)-P/C also exhibited better durability than Pt/C.[35]

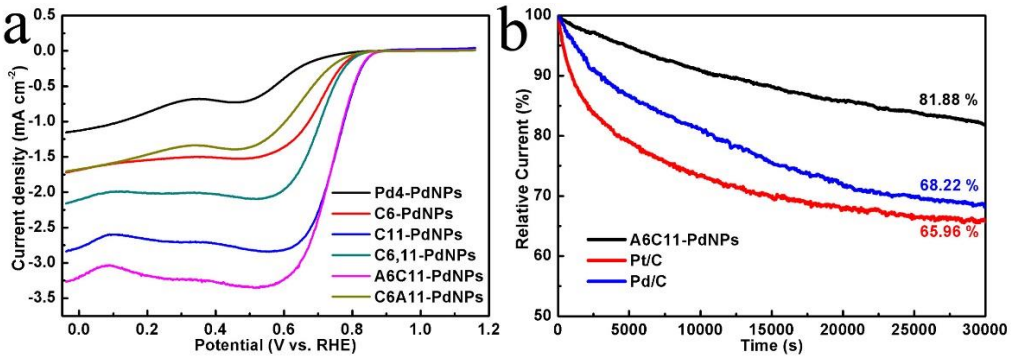

Figure 1. (a) Linear scanning voltammetric curves of a glassy carbon electrode coated with the six peptide-based PdNPs. (b) Chronoamperometric measurements for A6C11-PdNPs, Pd/C and Pt/C in an oxygen-saturated 0.1 M KOH aqueous solution for 30 000 s. Reproduced with permission,[25] copyright 2017 Elsevier B. V.

The peptide sequence can significantly affect the catalytic properties of the as-prepared noble metal nanomaterials, and through fine-tuning the amino acid residue, drastically different ORR performance can be achieved. One good example is Yang's study in 2017.[25] Yang *et. al* employed a series of peptides (including Pd4, C6, C11, C6,11, A6C11, C6A11) to fabricate six different Pd nanoparticles (PdNPs).[25] Pd4 peptide was employed as the parent sequence where the histidine residues at the 6th and/or 11th position were partially or fully substituted by cysteine and/or alanine residue to generate the other five sequences. Figure 1a presents the ORR performances of Pd4-, C6-, C11-, C6,11-, A6C11-, and C6A11-PdNPs. Notably, the onset potential and current density of these Pd NPs varied drastically with the peptide sequence, and A6C11-PdNPs held the most positive onset potential and the largest diffusion limited current density among the series. Furthermore, the durability of A6C11-PdNPs was compared with commercial Pd/C and Pt/C and evaluated by chronoamperometric responses (Figure 1b). After continuous test for 30 000 s, the A6C11-PdNPs modified electrode was able to maintain 81.88% of its initial current. Nonetheless, the currents of the electrode modified by Pd/C and Pt/C declined rapidly and preserved only 68.22% and 65.96% of the initial values in the end, respectively.

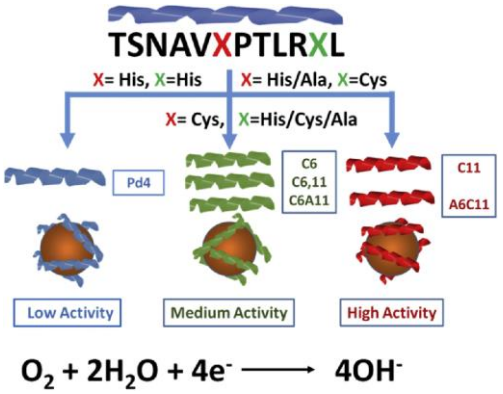

Scheme 1. The proposed mechanism regarding the effects of PdNPs capped by different peptide sequences for ORR. Reproduced with permission,[25] copyright 2017 Elsevier B. V.

It has been postulated that, the surface structure of the Pd NPs metal core is of great essence to the adsorption of oxygen molecule, which possibly governs the ORR process. Previous studies have shown that thiols hold robust binding interaction on the surface of noble metals, which can be employed for rational design for peptide capped nanoparticles with different catalytic behaviors.[36-38] Scheme 1 illustrates that a distinct tendency for ORR can be associated with the variation of peptide sequence. For the peptide sequences of A6C11 and C11, histidine close to the end of the sequence is substituted by cysteine (C) who possesses a thiol group. On the surface of A6C11-PdNPs and C11-PdNPs, it is probable that the ultra-strong binding interaction from cysteine adjacent to the terminal of the sequence emancipates the amino acid residues on the other side, allowing the maximal access for O_2 adsorption.[25] Such releasing effects exist but not so strong for C6-PdNPs, C6,11-PdNPs, and C6A11-PdNPs, while for parent sequence Pd4, there is no such effect. Consequently, the ORR performance followed a trend of A6C11-, C11- PdNPs > C6-, C6,11- and C6A11- PdNPs > Pd4-PdNPs. One can see that, by tuning one or two amino acid residues on the peptide sequence, significantly different ORR catalytic activities can be achieved, and a structure-property correlation has been successfully established.

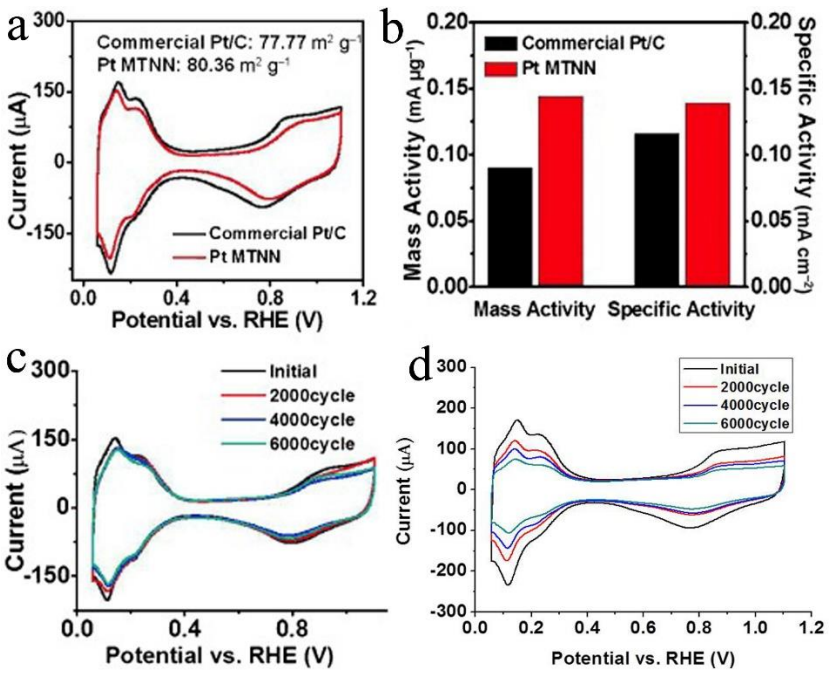

Figure 2. (a) The CV curves of Pt MTNN and Pt/C in the O_2-saturated 0.1 M $HClO_4$ solution with a scan rate of 50 mV s^{-1}. (b) The corresponding mass and specific activities of Pt MTNN and Pt/C at 0.9 V, respectively. The CV curves of (c) Pt MTNN and (d) Pt/C before and after the accelerated durability test. Reprinted with permission,[39] copyright 2013 John Wiley & Sons, Ltd.

In another hand, a variety of precious-metal-based nanocatalysts have been prepared by taking advantages of the self-assembly properties of the peptides. Beyond zero-dimensional nanoparticles, single noble metal materials with one-dimensional nanowire structure can also be acquired through peptide-mediated approach.[40] Thanks to the exposure of more active sites and acceleration of electron

transfer, nanowire may embrace better oxygen electroreduction ability than nanoparticles. One typical case is that, Huang group investigated the ultrathin Pt multiple-twinned nanowire network (MTNN), which showed higher electrochemically active surface area (EASA) and improved ORR activity compared with the Pt/C catalyst.[32, 39] The platinum MTNN was prepared by using a specific platinum-binding-peptide based amino acid sequence. Figure 2a depicts the CV curves with typical peaks related to hydrogen adsorption/desorption, and Pt MTNN possessed higher specific ECSA value than Pt/C.[39] As displayed in Figure 2b, Pt MTNN exhibited a mass activity of 0.144 mA μg^{-1}, distinctly higher than Pt/C (0.091 mA μg^{-1}). Despite the higher ECSA value, the specific activity of Pt MTNN was still higher than that of Pt/C. Furthermore, the accelerated durability test illustrates that Pt MTNN possessed exceptional stability and only a slight decay of the ECSA was observed after 6000 cycles (Figure 2c), while the ESCA of Pt/C decreased strikingly under the same operation conditions (Figure 2d).

Besides noble metal nanowire synthesized with the assistance of peptide, the peptide-templated two-dimensional nanofiber has also been gaining wide-spread attentions due to its potential various applications.[40, 41] In 2013, Jelinek *et. al* fabricated conductive and diaphanous Au nanofiber membranes on the surface of monolayer peptide.[42] After the peptide P_{FK}-5 assembled into nanofilms, a TEM grid was employed to carry the peptide film. Subsequently, the grid was submerged into an aqueous solution of $Au(SCN)_4^-$,[42] where the Au complexes with negative charge bound to the peptide film and were further reduced into metallic Au, resulting in the formation of the nanofiber networks of gold.[42] It can be noted that, using peptide as template can open a new avenue for preparing single noble metal materials with 2D structure. Nonetheless, the process of peptide being self-assembled into nanofilms requires prolonged operation time, which strictly restricts the promotion and widespread application of such method.[40] Using organic substrate can save the time, but the corresponding electrochemical performance of the catalyst may be affected and weakened.[40] Therefore, it is meaningful and imperative for exploring other new strategies to more efficiently prepare such material.

2.2 Peptide-based alloyed bimetallic nanomaterials for ORR

Similar to single noble metal capped with peptide, the binary alloys, including AuAg, AuPd, AuPt, and other bimetallic nanoparticles, capped or templated by the peptide sequences, have also received wide attentions recently.[28, 43, 44] Compared with single noble metal, alloying can crucially adjust the electronic structure and the atomic ordering pattern of the catalysts, hence playing a critical role in the electrochemical process.[45] Alloying a catalytically active metal to another metal can improve the surface reactivity by crippling binding oxygen atoms while readily breaking the O=O bond.[45] Furthermore, owing to the introduction of additional synergistic effect, plus the ligand effect, excellent performance and excellent stability can be probably acquired from alloyed bimetallic nanoparticles.

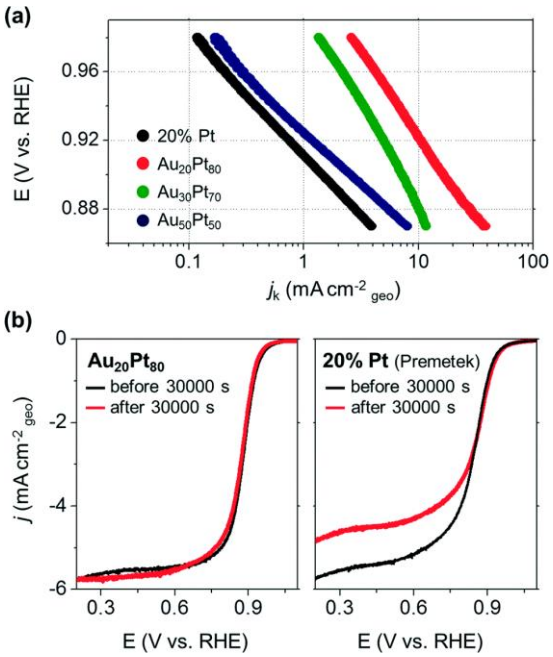

Figure 3. Electrochemical analysis of the Au_xPt_{100-x}/HC/SWNT samples and Pt/C: (a) Tafel plots; (b) ORR polarization curves before and after 30 000 s cycles at the potential of 0.4 V. The polarization curves of the catalysts were acquired on a rotating disk electrode in an O_2-saturated 0.1 M KOH aqueous solution at a scanning rate of 10 mV s^{-1} and a rotation rate of 1600 rpm. Reproduced with permission,[45] copyright 2016 Royal Society of Chemistry.

In 2016, Kim group documented the synthesis of surface-component-dominated AuPt nanoparticles on single-walled carbon nanotube (SWNT) by peptide-derived self-assembly and their electrochemical responses to oxygen reduction.[45] In this study, the surface of AuPt NPs coated by the peptide had at least three highlights: (1) crystallization of nanoparticles along the SWNT axis, (2) adjustment onto the ratio of Au and Pt without pyrolysis or high temperature treatment, and (3) formation of size-selective nanoparticles without any other capping ligands.[45] The Au_xPt_{100-x}/HC/SWNT (x denotes the molar percentage, where x = 20, 30, 50) displayed increased ORR performance, which was intently related to the surface composition ratio of the AuPt NPs. As for the Au_xPt_{100-x}/HC/SWNT series, the Tafel slopes of the samples with different Au/Pt ratios are shown in Figure 3a to evaluate the ORR intrinsic reaction kinetics. The Tafel plots manifested that the ORR kinetics of Au_xPt_{100-x}/HC/SWNT was superior to that of Pt/C, and $Au_{20}Pt_{80}$/HC/SWNT exhibited the highest ORR inherent dynamic rate among the series. Moreover, Figure 3b clarifies that the long term durability of $Au_{20}Pt_{80}$/HC/SWNT was obviously better than that of Pt/C, suggesting the Pt surfaces were stabilized against dissolution or corrosion owing to the protection of the surrounding Au atoms. This stabilization effect of Au claimed that peptide can serve as effective template for constructing stable bimetallic nanostructures.[45]

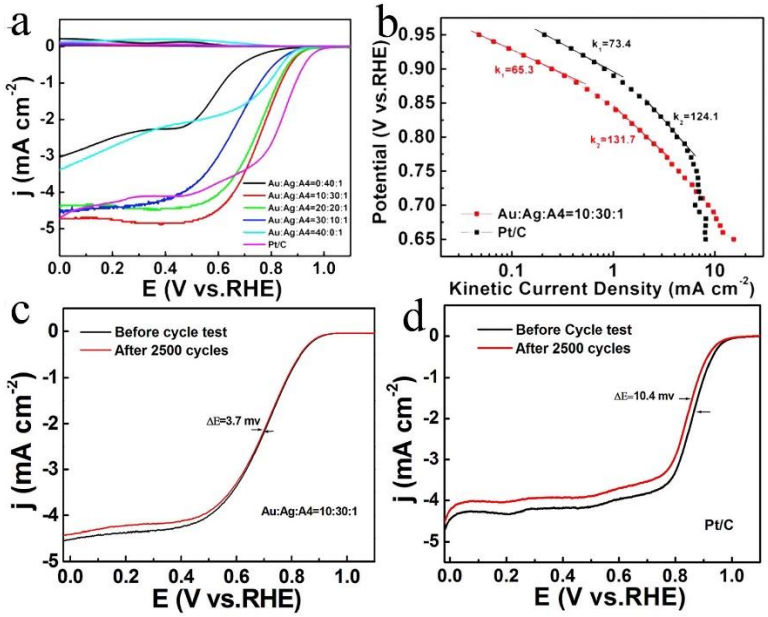

Figure 4. The ORR performance of the samples with different Au-to-Ag ratio and definite alloy-to-peptide ratio (40: 1) and Pt/C in oxygen-saturated 0.1 M KOH aqueous solution: (a) linear scanning curves; (b) the corresponding Tafel plots of Au: Ag: A_4 = 10: 30: 1 and Pt/C. The ORR polarization curves of Au: Ag: A_4 = 10: 30: 1 (c) and Pt/C (d) before and after 2500 cycles between 0.6 and 1.0 V at a scan speed of 50 mV $^{-1}$ with a rotation rate of 1600 rpm. Reproduced with permission, copyright 2017 Elsevier B. V.[44]

Also, a series of peptide-A4-based AuAg alloys were fabricated by Tang group to evaluate the oxygen reduction performance.[44] Among the Au: Ag : A_4 = x: 40-x: 1 (x denotes the molar ratio, where x= 0, 10, 20, 30, 40) series, Au: Ag: A_4 = 10: 30: 1 embraced the most positive onset potential (0.94 V) and the largest diffusion-limited current density (4.87 mA cm^{-2}), where the onset potential approached that of commercial Pt/C (0.95 V), and diffusion-limited current density was larger than Pt/C (4.67 mA cm^{-2}) (Figure 4a).[44] Moreover, the Tafel slopes of Au: Ag: A_4 = 10: 30: 1 and Pt/C are shown in Figure 4b, where similar features and approximative Tafel slope values can be obtained for Au: Ag: A_4 = 10: 30: 1 (65.3 mV dec^{-1}, 131.7 mV dec^{-1}) and Pt/C (73.4 mV dec^{-1}, 124.1 mV dec^{-1}), revealing that the rate-determining step in the low-potential window may be a pseudo-two-electron-transfer process, and the reaction rate was governed by the first electron transfer to O_2 in high-potential window.[44] Finally, Figures 4c and 4d illustrate the accelerated durability test results of Au: Ag: A_4 = 10: 30: 1 and Pt/C by cycling the catalyst in the potential range from +0.6 to +1.0 V.[44] The half wave potential shifted negatively of 10.4 mV for Pt/C after 2500 cycles, while only 3.7 mV shift was observed for Au: Ag: A_4= 10: 30: 1, attesting that Au: Ag: A_4 = 10: 30: 1 held better stability than Pt/C under the same conditions. Such exceptional activity and durability were attributed to the two factors: (1) The strong ensemble electronic interaction between the Au and Ag atoms imparted synergistic effects, which were beneficial to the kinetics process of ORR; (2) Peptide A4 acted as protecting agent, which hindered the AuAg bimetallic nanoparticles from severe corrosion, coalescence and aggregation.[44]

2.3 Peptide-based core-shell bimetallic nanomaterials for ORR

In the last decade, bimetallic noble metal nanostructures with core-shell architecture have been receiving mounting research interests, mainly due to their multifarious applications in catalysis, electrocatalysis, optics, electronic, sensing, and so forth.[46, 47] It is worth noting that, core-shell structures often exhibit improved electrochemical properties owing to the created lattice strain between the core and the shell, along with the catalytic synergistic effects in the electrocatalytic process.[48, 49] Through rational design, core-shell nanostructure can be created by introducing specific peptide sequence during the preparation.

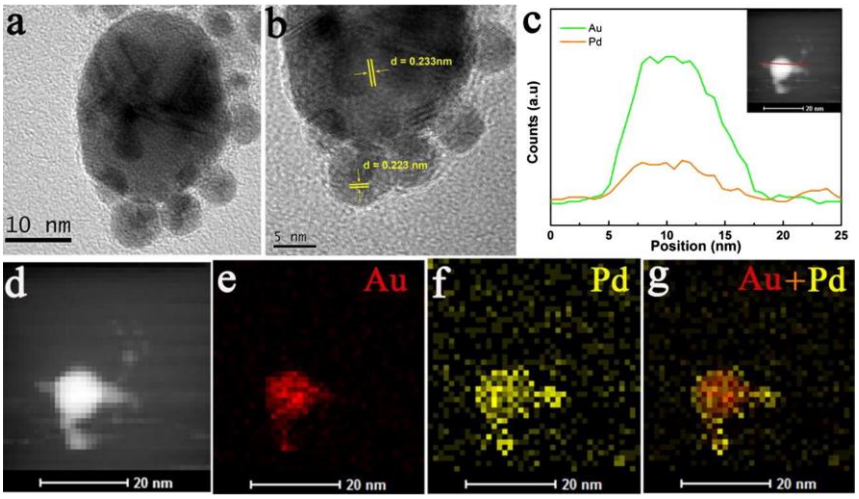

Figure 5. (a) Representative TEM image (a) and HR-TEM image (b) of the Au@$Pd_{1.0}$ sample. Cross-section line-scan profile (c) of Au@$Pd_{1.0}$ (inset: a typical HAADF-STEM image). Representative black field (BF)-STEM image (d) of the Au@$Pd_{1.0}$ sample and the EDX elemental mapping of Au (e), Pd (f) and Au + Pd (g) elements in the Au@$Pd_{1.0}$ sample. Reproduced with permission,[50] copyright 2018 Elsevier B. V.

In 2018, Zong *et. al* reported the fabrication of an Au nanoparticle inside Pd nanoparticles outside core@shell structure for both hydrogen evolution and ORR.[50] The sequence employed was FlgA3, which contains two domains of A3 and Flg. The A3 domain holds binding sites to Au surface and can form stable Au nanoparticles, while the Flg domain has strong binding interaction with Pd surface.[51, 52] Through sequential reduction, the Au@Pd_x (x denotes the Pd-to-Au molar ratio, x = 0.17, 0.50, 1.0 and 1.5) series was prepared.[50] The core-shell structure of the Au-Pd bimetallic nanomaterials can be verified by the electron microscopy techniques (Figure 5). From Figure 5a and 5b, it can be noted that one large Au particle is inside while several Pd nanoparticles are partially covered on the surface of the particle, suggesting a special Au-particle@Pd-nanoparticles core@shell structure was formed. The line-scan profile in Figure 5c demonstrates that the Au elemental concentration is peak-shaped, while Pd has somewhat higher concentration at the edges. From the drift corrected image in Figure 5d and the elemental mappings in Figures 5e-5g, one can see that the Au elements locate in the center while the Pd

elements are mainly around onto the outside. It verifies the successful preparation of a core-shell architecture.

Table 1. Summary of the ORR properties of the Au@Pd_x series in 0.1 M KOH. Reproduced with permission,[50] copyright 2018 Elsevier B. V.

Sample	$E_{1/2}$ (V vs. RHE)	Diffusion limited current (mA cm^{-2})	Number of electron transferred (n)
Au@$Pd_{0.17}$	0.58	2.76	1.68–3.54
Au@$Pd_{0.5}$	0.71	2.49	3.66–3.77
Au@$Pd_{1.0}$	0.85	4.91	3.91–3.96
Au@$Pd_{1.5}$	0.83	4.47	3.82–3.95
Pt/C	0.82	5.01	3.81–3.86
Pd/C	0.78	5.71	3.41–3.87

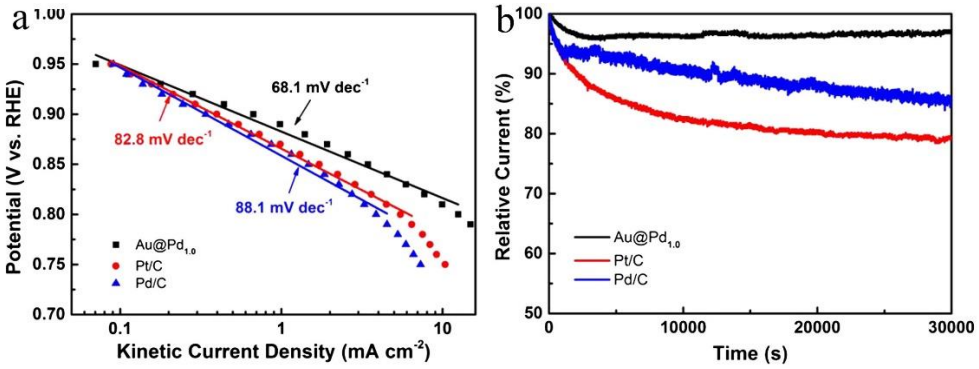

Figure 6. (a) The Tafel slope values for Au@$Pd_{1.0}$, Pd/C, and Pt/C at the low-overpotential range. (b) Long-term stability test of Au@$Pd_{1.0}$, Pd/C and Pt/C in the O_2-saturated 0.1 M KOH aqueous solution with a rotation rate of 900 rpm. Reproduced with permission,[50] copyright 2018 Elsevier B. V.

The electrocatalytic performance of the Au@Pd_x series is shown in Figure 6 and compiled in Table 1 as well. With the increasing of Pd-to-Au ratio, the performance of the Au@Pd_x series first enhanced and then decreased, and Au@$Pd_{1.0}$ held the best ORR activity with the highest half-wave potential, the largest diffusion-limited current and most efficient direct 4e pathway (Table 1).[50] In addition, the onset potential of Au@$Pd_{1.0}$ was larger than Pd/C and Pt/C, and the corresponding Tafel slopes were calculated to be 68.1 mV dec^{-1}, 88.1 mV dec^{-1}, and 82.8 mV dec^{-1} for Au@$Pd_{1.0}$, Pd/C, and Pt/C (Figure 6a), respectively. The long-term durability of Au@$Pd_{1.0}$ for ORR was also compared with Pd/C and Pt/C by chronoamperometric *i-t* test. As illustrated in Figure 6b, the Au@$Pd_{1.0}$ modified electrode can maintain 96.5% of its initial current after continuous operation for 30 000 s. Nevertheless, the currents of the electrode decorated by Pd/C and Pt/C declined rapidly and finally preserved only 85% and 80% of the initial values, respectively. The results implied that peptide-based core-shell structure of Au-nanoparticle@Pd-nanoparticles maintained an exceedingly higher long-term stability than Pd/C and Pt/C for ORR in alkaline solution.

3. CONCLUSION AND PERSPECTIVE

In the past a few years, great research endeavors have been dedicated to electrochemical oxygen reduction due to its great implications for sustainable energy conversion and storage technologies, such as PEMFCs, RMABs, and so forth. Nevertheless, the lack of high-efficiency, relatively-cheap electrocatalysts with superior stability and durability tremendously hampers the advancement and deployment of these green energy devices. Notably, it may promote the syntheses of catalysts toward ORR by using biomolecules, such as protein, DNA, specially peptide sequence, as a template. Particularly, the above-mentioned research efforts have affirmed that peptides can direct the formation of catalysts with desirable shape, size, orientation, structure and composition under mild conditions. Impressively, most of these peptide-derived noble metal nanomaterials exhibited comparable oxygen reduction activity to Pt/C, and the long-term durability of these nanomaterials were clearly better than Pt/C. The peptide-templated approach can shed light on fabricating noble metal nanomaterial with great potentials employed in electrochemical energy regime.

However, there are still some obstacles that restrict large-scale applications of peptide-based noble metal nanomaterials. Firstly, these peptide sequences are either laboratory-synthesized or manufactured through industrial plants, and the associated high cost would be a big ineluctable issue; Secondly, it requires further enrichment and consummation for the library of peptide sequences with specific binding affinities on different metal substrates. Currently, the peptide sequences with specific targeting capabilities are still limited, where machine learning and artificial intelligent technologies may play an important role for screening the desirable sequences.

It is envisioned that, the establishment of peptide/polypeptide/protein multi-hierarchical structure that permits the usage of a wide variety of inorganic materials will be of much benefit to simplify the synthesis process. Finally, substituting expensive noble metals with inexpensive transition metals can decrease the cost of nanomaterials and facilitate these catalysts being commercialized and practically employed more smoothly and conveniently. Overall, we anticipate that peptide-based noble metal nanomaterials will embrace a prospective promise with both challenges and opportunities.

ACKNOWLEDGEMENTS

W. H. is grateful for the financial support from Science and Technology Program of Chongqing Teaching Committee (No. KJ1604301), Z. T. thanks the financial support from Guangdong Innovative and Entrepreneurial Research Team Program (No. 2014ZT05N200).

References

1. B. Han, C. E. Carlton, A. Kongkanand, R. S. Kukreja, B. R. Theobald, L. Gan, R. O'Malley, P. Strasser, F. T. Wagner, Y. Shao-Horn, *Energy Environ. Sci.*, 8 (2015) 258.
2. J. Yi, P. Liang, X. Liu, K. Wu, Y. Liu, Y. Wang, Y. Xia, J. Zhang, *Energy Environ. Sci.*, 11 (2018) 3075.
3. Z. Ding, Z. Tang, L. Li, K. Wang, W. Wu, X. Chen, X. Wu, S. Chen, *Inorg. Chem. Front.*, 5 (2018) 2425.
4. M. Shao, Q. Chang, J.-P. Dodelet, R. Chenitz, *Chem. Rev.*, 116 (2016) 3594.

5. K. Wang, Z. Tang, W. Wu, P. Xi, D. Liu, Z. Ding, X. Chen, X. Wu, S. Chen, *Electrochim. Acta,* 284 (2018) 119.
6. Y. Nie, L. Li, Z. Wei, *Chem. Soc. Rev.,* 44 (2015) 2168.
7. K. Wang, W. Wu, Z. Tang, L. Li, S. Chen, N. M. Bedford, *ACS Appl. Mater. Interfaces,* 11 (2019) 4983.
8. H.-W. Liang, W. Wei, Z.-S. Wu, X. Feng, K. Müllen, *J. Am. Chem. Soc.,* 135 (2013) 16002.
9. Z. Ding, K. Wang, Z. Mai, G. He, Z. Liu, Z. Tang, *Int. J. Hydrogen Energy,* 44 (2019) 24680.
10. Z. Qian, Y. Chen, Z. Tang, Z. Liu, X. Wang, Y. Tian, W. Gao, *Nano-Micro Lett.,* 11 (2019) 28.
11. D. Guo, R. Shibuya, C. Akiba, S. Saji, T. Kondo, J. Nakamura, *Science,* 351 (2016) 361.
12. W. Yan, Z. Tang, L. Wang, Q. Wang, H. Yang, S. Chen, *Int. J. Hydrogen Energy,* 42 (2017) 218.
13. A. Kulkarni, S. Siahrostami, A. Patel, J. K. Nørskov, *Chem. Rev.,* 118 (2018) 2302.
14. Z. Tang, W. Wu, K. Wang, *Catalysts,* 8 (2018) 65.
15. J. Masa, W. Xia, M. Muhler, W. Schuhmann, *Angew. Chem., Int. Ed.,* 54 (2015) 10102.
16. Y. Jiao, Y. Zheng, M. Jaroniec, S. Z. Qiao, *Chem. Soc. Rev.,* 44 (2015) 2060.
17. C. M. Sánchez-Sánchez, A. J. Bard, *Anal. Chem.,* 81 (2009) 8094.
18. L. Yu, X. Pan, X. Cao, P. Hu, X. Bao, *J. Catal.,* 282 (2011) 183.
19. L. Wang, Z. Tang, W. Yan, Q. Wang, H. Yang, S. Chen, *J. Power Sources,* 343 (2017) 458.
20. T. Li, Y. Chen, Z. Tang, Z. Liu, C. Wang, *Electrochim. Acta,* 307 (2019) 403.
21. T. Li, Z. Tang, K. Wang, W. Wu, S. Chen, C. Wang, *Int. J. Hydrogen Energy,* 43 (2018) 4932.
22. B.-A. Lu, T. Sheng, N. Tian, Z.-C. Zhang, C. Xiao, Z.-M. Cao, H.-B. Ma, Z.-Y. Zhou, S.-G. Sun, *Nano Energy,* 33 (2017) 65.
23. Q. Sun, C. Sun, A. Du, S. Dou, Z. Li, *Nanoscale,* 8 (2016) 14084.
24. H. Yang, C. Wen, Z. Tang, L. Wang, Q. Wang, W. Yan, W. Wu, S. Chen, *J. Mater. Sci.,* 52 (2017) 8016.
25. H. Yang, Z. Tang, W. Yan, L. Wang, Q. Wang, Y. Zhang, Z. Liu, S. Chen, *J. Alloys. Compd.,* 702 (2017) 146.
26. M. B. Dickerson, K. H. Sandhage, R. R. Naik, *Chem. Rev.,* 108 (2008) 4935.
27. B. D. Briggs, M. R. Knecht, *J Phys Chem Lett,* 3 (2012) 405.
28. W. Wu, Z. Tang, K. Wang, Z. Liu, L. Li, S. Chen, *Electrochim. Acta,* 260 (2018) 168.
29. T. R. Walsh, M. R. Knecht, *Chem. Rev.,* 117 (2017) 12641.
30. S. Chattopadhyay, A. Sarkar, S. Chatterjee, A. Dey, *J. Mater. Chem. A,* 6 (2018) 1323.
31. J. Wang, S. Kattel, Z. Wang, J. G. Chen, C.-J. Liu, *ACS Appl. Mater. Interfaces,* 10 (2018) 21321.
32. Y. Li, Y. Huang, *Adv. Mater.,* 22 (2010) 1921.
33. K. R. Lee, E. S. Kang, Y.-T. Kim, N. H. Kim, D. Youn, Y. D. Kim, J. Lee, Y. H. Kim, *Catal. Today,* 295 (2017) 95.
34. N. A. Merrill, T. T. Nitka, E. M. McKee, K. C. Merino, L. F. Drummy, S. Lee, B. Reinhart, Y. Ren, C. J. Munro, S. Pylypenko, A. I. Frenkel, N. M. Bedford, M. R. Knecht, *ACS Appl. Mater. Interfaces,* 9 (2017) 8030.
35. W. Wang, Z. Wang, M. Yang, C.-J. Zhong, C.-J. Liu, *Nano Energy,* 25 (2016) 26.
36. F. J. Ibañez, F. P. Zamborini, *Langmuir,* 22 (2006) 9789.
37. R. Coppage, J. M. Slocik, B. D. Briggs, A. I. Frenkel, H. Heinz, R. R. Naik, M. R. Knecht, *J. Am. Chem. Soc.,* 133 (2011) 12346.
38. R. Coppage, J. M. Slocik, H. Ramezani-Dakhel, N. M. Bedford, H. Heinz, R. R. Naik, M. R. Knecht, *J. Am. Chem. Soc.,* 135 (2013) 11048.
39. L. Ruan, E. Zhu, Y. Chen, Z. Lin, X. Huang, X. Duan, Y. Huang, *Angew. Chem., Int. Ed.,* 52 (2013) 12577.
40. W. Wang, C. F. Anderson, Z. Wang, W. Wu, H. Cui, C.-J. Liu, *Chem. Sci.,* 8 (2017) 3310.
41. B. G. Choi, M. H. Yang, T. J. Park, Y. S. Huh, S. Y. Lee, W. H. Hong, H. Park, *Nanoscale,* 3 (2011) 3208.
42. T. P. Vinod, S. Zarzhitsky, A. Morag, L. Zeiri, Y. Levi-Kalisman, H. Rapaport, R. Jelinek,

Nanoscale, 5 (2013) 10487.
43. D. Li, Z. Tang, S. Chen, Y. Tian, X. Wang, *ChemCatChem*, 9 (2017) 2980.
44. Q. Wang, H. Yang, Z. Zhou, L. Wang, W. Yan, W. Wu, S. Chen, Z. Liu, Z. Tang, *Int. J. Hydrogen Energy*, 42 (2017) 11295.
45. Y.-S. Ko, Y.-T. Kim, J.-H. Kim, D. H. Kim, K.-H. Kim, W. S. Yun, Y. D. Kim, J. Lee, Y. H. Kim, *CrystEngComm*, 18 (2016) 6024.
46. K. D. Gilroy, A. Ruditskiy, H.-C. Peng, D. Qin, Y. Xia, *Chem. Rev.*, 116 (2016) 10414.
47. W. Wang, B. Lei, S. Guo, *Adv. Energy Mater.*, 6 (2016) 1600236.
48. D. Chen, C. Li, H. Liu, F. Ye, J. Yang, *Sci. Rep.*, 5 (2015) 11949.
49. G. Yang, D. Chen, P. Lv, X. Kong, Y. Sun, Z. Wang, Z. Yuan, H. Liu, J. Yang, *Sci. Rep.*, 6 (2016) 35252.
50. Z. Zong, K. Xu, D. Li, Z. Tang, W. He, Z. Liu, X. Wang, Y. Tian, *J. Catal.*, 361 (2018) 168.
51. J. M. Slocik, M. O. Stone, R. R. Naik, *Small*, 1 (2005) 1048.
52. J. M. Slocik, R. R. Naik, *Adv. Mater.*, 18 (2006) 1988.